Supporting information for

"Rigid-flexible" dynamic polymers based on borate bonds

*Jing Tu[1], Bo Chen[1], Xinhong Xiong[1], Weiming Xu[2], JiaXi Cui[1,2]**

[1] Yangtze Delta Region Institute (Huzhou), University of Electronic Science and Technology of China, Huzhou 313001 (P. R. China)

[2] Institute of Fundamental and Frontier Sciences, University of Electronic Science and Technology of China, Chengdu 610054, (P. R. China)

E-mail: Jiaxi.Cui@uestc.edu.cn

Materials

3-Mercaptopropane-1,2-diol (98%, Adamas), 1,4-benediboronic acid (98%, Adamas), 3,6-dioxa-1,8-octanedithiol (98%, Adamas), 3,6-dioxa-1,8-octanedithiol (97%, Adamas), triallyl isocyanurate (99%, Adamas), photoinitiator I-819 (99%, Adamas), magnesium sulfate (99%, J&K Scientific), tetrahydrofuran (99%, Aladdin), dichloromethane (99%, Aladdin) were used as purchased.

Synthesis of 2,2'-(1,4-phenylene)-bis[4-mercaptan-1,3,2-dioxaborolane] (BDB)

The BDB was synthesized from the coupling reaction between 3-mercaptopropane-1,2-diol with benzene-1,4-diboronic acid. Briefly, benzene-1,4-diboronic acid (6.0 g) and

3-allyloxy-1,2-propanediol (8.0 g) were dissolved in tetrahydrofuran (150 mL) and water (0.15 mL), and to which magnesium sulfate (10.0 g) was added. After stirring at room temperature for 24 h, the mixture was filtered and washed with methylene chloride to obtain the white powder target compound. The chemical structure of BDB was confirmed via ^{1}H NMR spectroscopy (Figure S1).

Typical Synthesis Procedure of TAIC-DB (TAIC-DT)

Take TAIC-DB as an example. BDB (3.78 g), photoinitiator I-819 (200 mg), and Triallyl isocyanurate (2.00 g) were mixed and heated to melt at 100°C. After all the solids were dissolved, a yellow viscous liquid was obtained. The mixed viscous liquid was then quickly poured into Teflon mold and sent to light-curing chamber. After curing for 1.5 h, a yellowish glassy sample was obtained. Synthesis procedure of TAIC-DT was same as that of TAIC-DB, except that it did not need to be heated for melting.

Instrumentation and Analysis

H-NMR spectra was recorded on a Bruker ARX 300 instrument using DMSO as the solvent.

Thermo Fisher's Nicolet IS-10 Fourier Transform Infrared spectrometer (FTIR) was used to test FT-IR spectra in the range of 400–4000 cm^{-1}.

The crystalline phase of the samples was determined by Rigaku Smartlab X-ray diffractometer (XRD) with Cu Kα radiation (λ = 0.15406 nm).

The thermal decomposition process of samples was measured by TA Discovery SDT

650 (TG-DSC) in the temperature range of 50-600°C under N_2 atmosphere where the heating rate was 10 °C/min.

The self-healing process of sample scratches and detail of fingerprints were observed by Soptop RX50M optical microscope system.

Tensile tests were performed at room temperature using Jinan Wenteng WDW-B instrument with a 500 N sensor at different deformation rates (2 mm/min, 5 mm/min, 10 mm/min, 50 mm/min). The modulus was calculated by the slope between the stress and the strain in the strain ranges of 1%−2%.

DMA tester (Q800 DMA, TA Instruments) was employed to characterize the thermomechanical properties in the stretch mode. Samples with the dimension of 50 mm × 5.0 mm × 2.0 mm were tested at a frequency of 1 Hz and a vibration amplitude of 0.1%. The sample was kept at -30°C for 5 min firstly, and then increased to 65°C at a heating rate of 3 °C/min. The glass transition temperatures (Tg) were confirmed by the turning point of the storage modulus. The frequency field scan-relaxation ability test of the sample was performed with a vibration amplitude of 0.1% and gradually decreased from 100 Hz until the relaxation crosslink appeared.

Stress relaxation tests were also performed at the DMA tester (Q800 DMA, TA Instruments) under stretch mode. The samples were first kept at the corresponding temperature for 3 min, then tested with a vibration amplitude of 0.1%. Creep tests were tested by DMA tester (Q800 DMA, TA Instruments) too. The test was carried out at a fixed stress of 0.1MPa at the corresponding temperature.

Supporting images

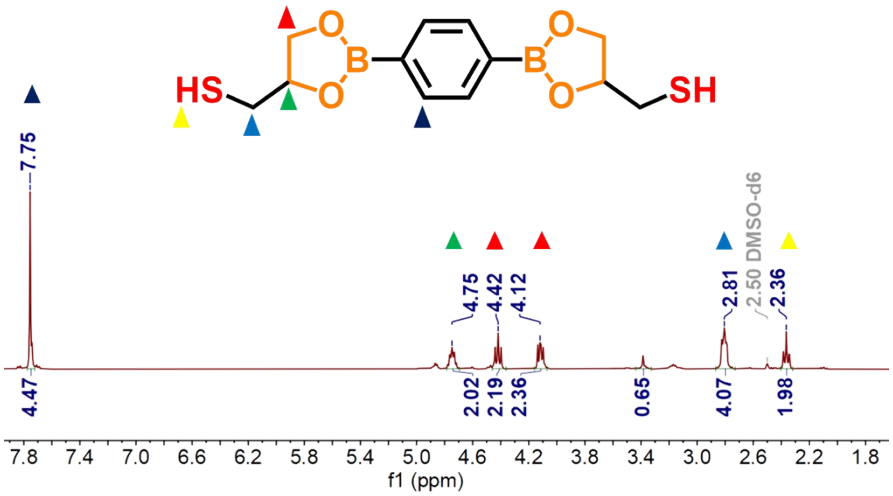

Figure S1 H-NMR spectra of BDB

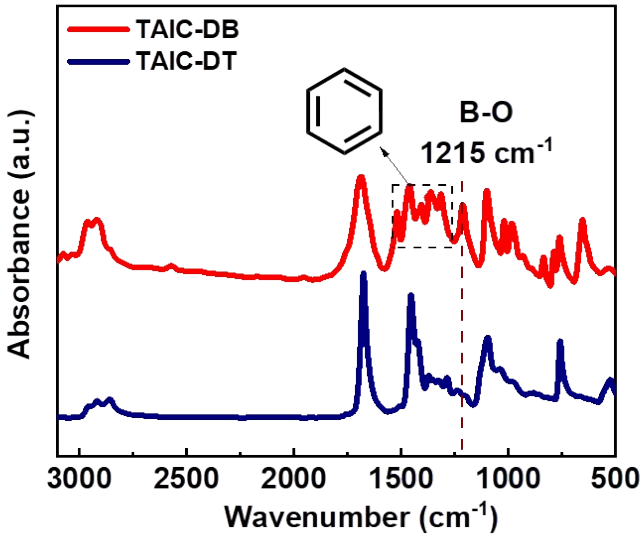

Figure S2 The FTIR spectras of the samples

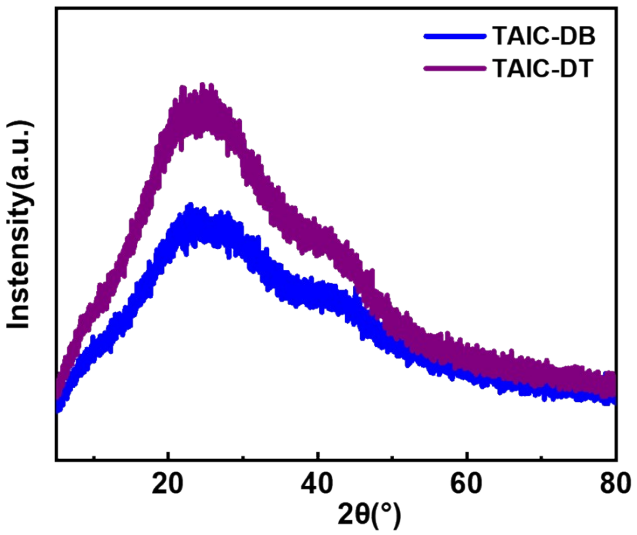

Figure S3 XRD spectra of TAIC-DB and TAIC-DT

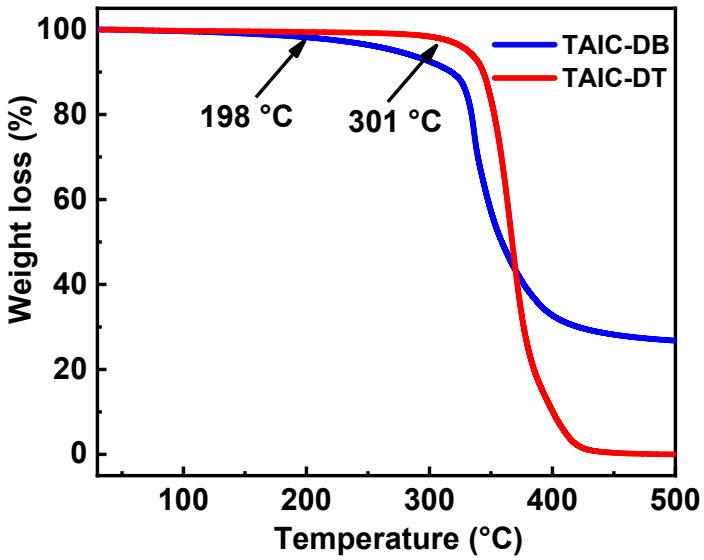

Figure S4 TGA curve of TAIC-DB and TAIC-DT

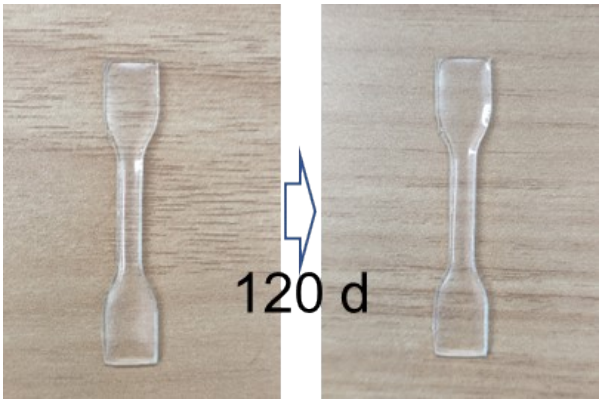

Figure S5 Structural stability of Rigid-flexible crosslink polymers TAIC-DB

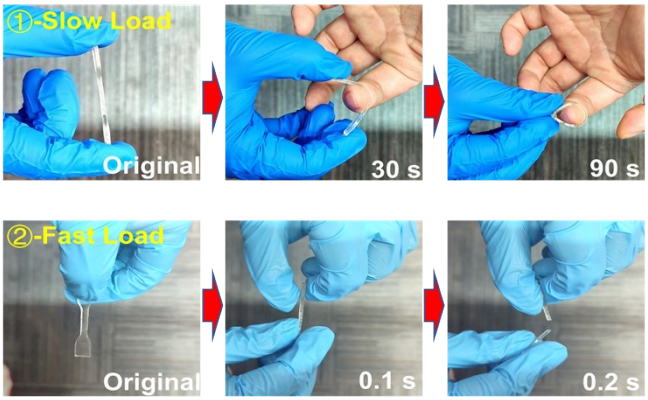

Figure S6 Rigidity and flexibility characteristics of TAIC-DB at different load rates

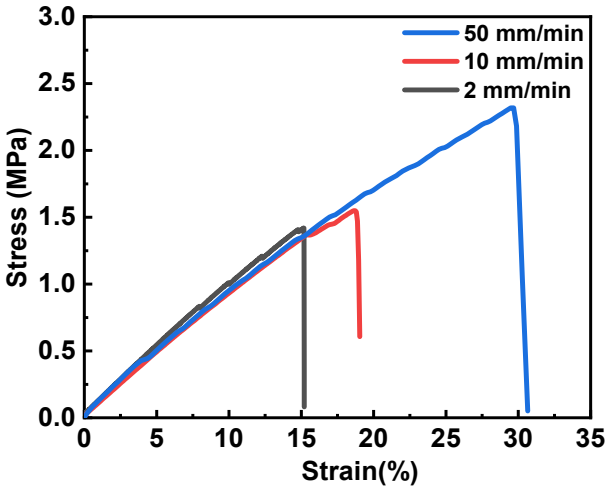

Figure S7 Stress-strain curves of TAIC-DT at different tensile rates

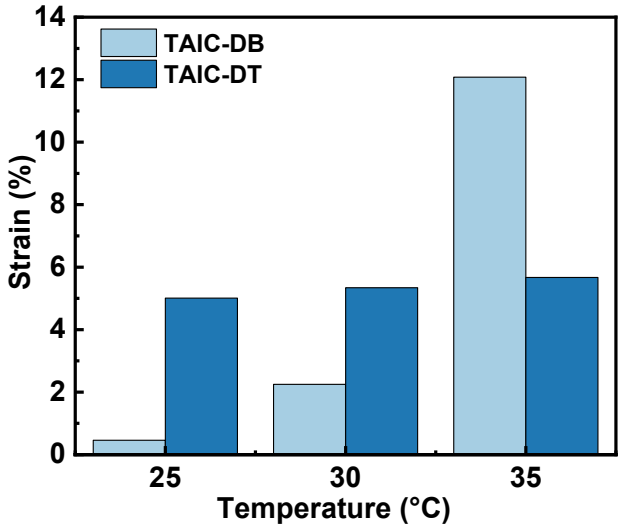

Figure S8 Comparison of creep properties of two samples over a period of 100 seconds

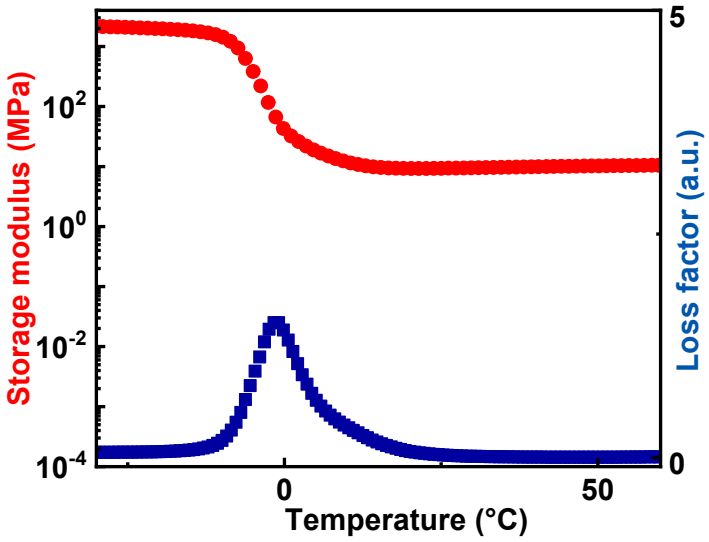

Figure S9 The temperature dependence of modulus and loss factor for TAIC-DT

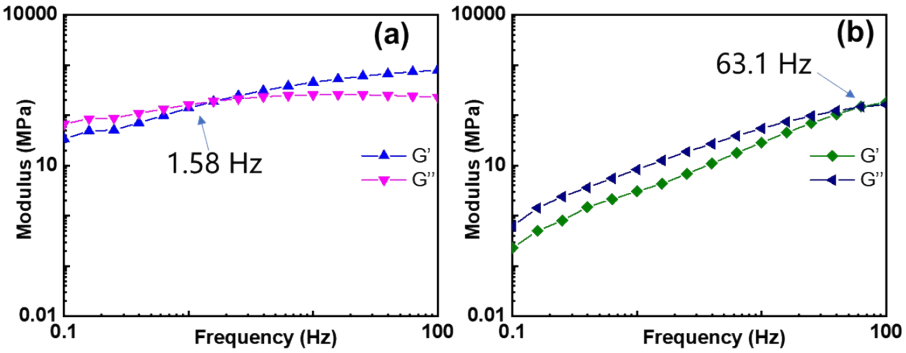

Figure S10 (a) Frequency dependence of modulus for TAIC-DB at 35℃; (b) Frequency dependence of modulus for TAIC-DB at 50℃

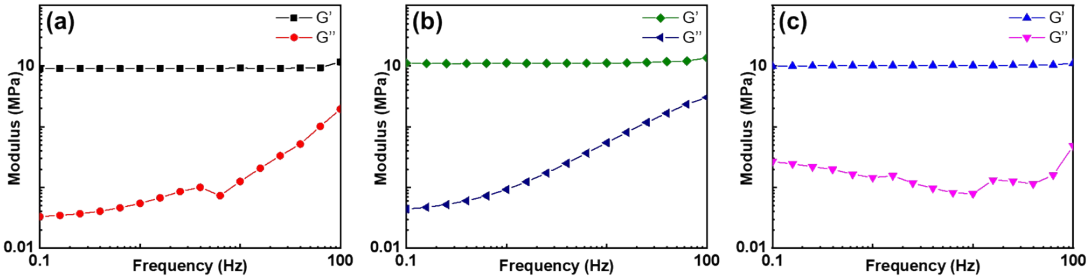

Figure S11 (a) Frequency dependence of modulus for TAIC-DT at 25℃; (b) Frequency dependence of modulus for TAIC-DT at 35℃; (b) Frequency dependence of modulus for TAIC-DT at 50℃

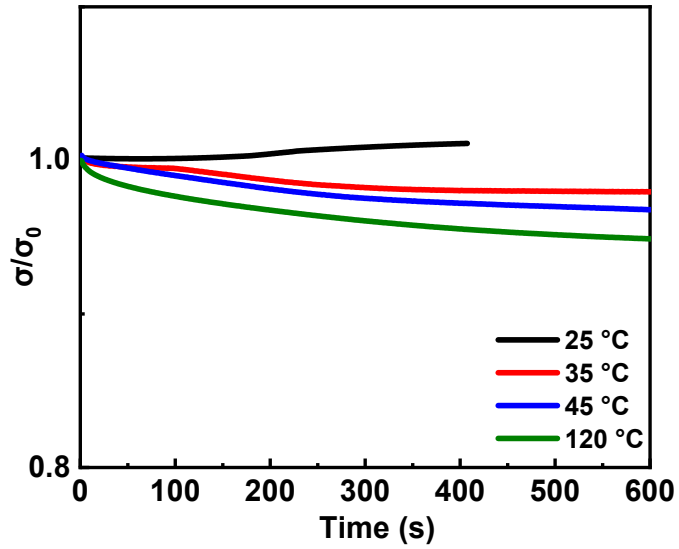

Figure S12 Stress relaxation curves of TAIC-DT at different temperatures

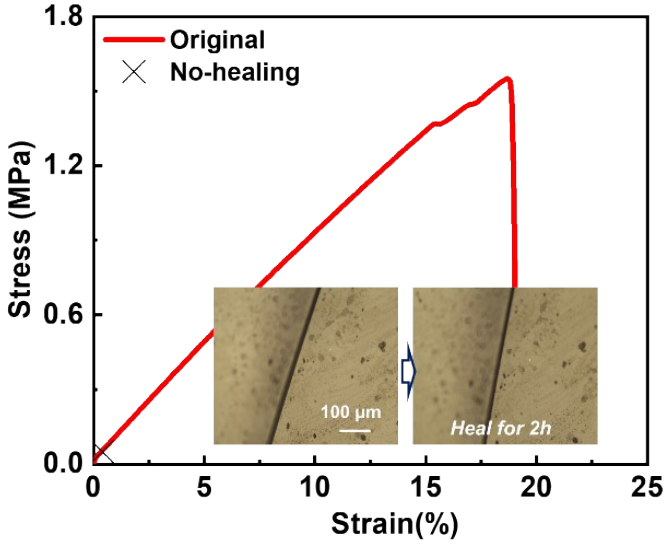

Figure S13 The self-heal performance of TAIC-DT

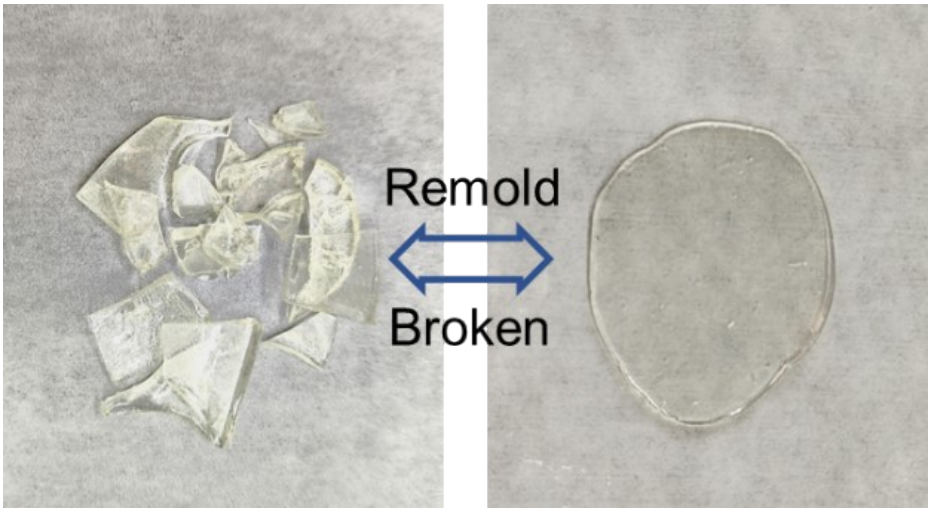

Figure S14 The remold performance of TAIC-DB

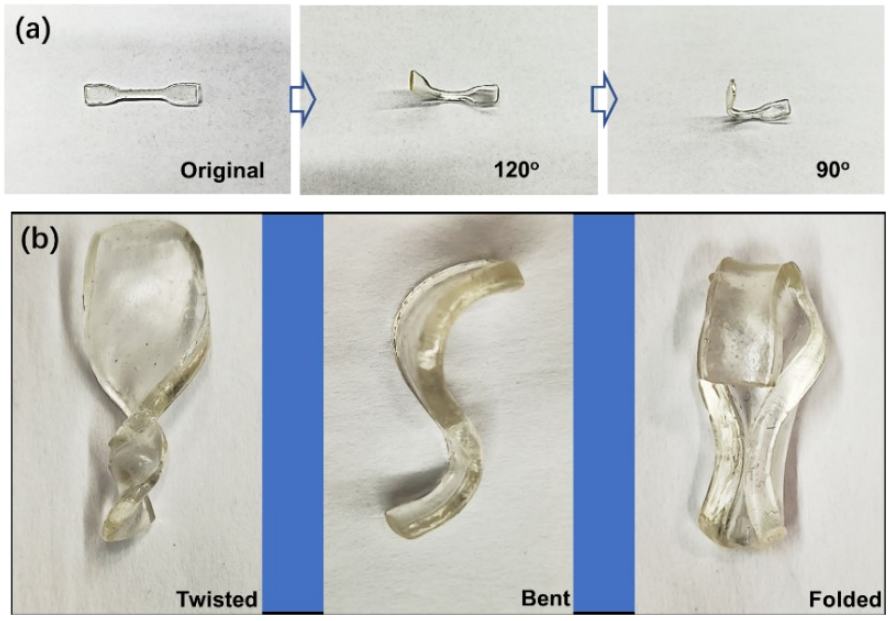

Figure S15 The programing performance of TAIC-DB at room temperature. (a) Bending ability; (b) Shape editing capabilities